

## New compensation method for Lock-in thermography to eliminate lateral heat flux

by J. Hufert\*, J. Rittmann\*\* and M. Kreutzbruck\*

\* Institut für Kunststofftechnik, University of Stuttgart, Pfaffenwaldring 32, 70569 Stuttgart, Germany, [jonas.hufert@ikt.uni-stuttgart.de](mailto:jonas.hufert@ikt.uni-stuttgart.de)

\*\* Precitec GmbH & Co. KG, Draisstr. 1, 76571 Gaggenau-Bad Rotenfels, Germany

### Abstract

Active thermography is a non-destructive testing method for material characterization and layer thickness measurement. The response of a thermal wave is monitored and evaluated by means of a thermographic camera. The diffusive properties of the thermal wave cause a lateral propagation of the thermal wave and limit the spatial resolution as well as the detection of defects. In this work, a method for reducing lateral heat fluxes in optical lock-in thermography is demonstrated. The lock-in thermography compensation method leads to higher edge sharpness, better separability of multiple defects as well as increased defect detection with increased SNR by the factor of 5.

### 1. Introduction

The active thermography (AT) uses heat to detect internal defects in structures. Lock-in thermography (LT) uses sine wave modulated heating to analyse structures phase wise. The heat is induced on the surface of the structure and spreads out into the structure. When inhomogeneities like defects or geometrical properties occur, the spreading heat is reflected differently regarding the homogeneous regions. These reflections can be detected on the surface of the structure by a difference in surface temperature using an IR camera.

Because heat spreads evenly in all directions, reflected heat of inhomogeneities occur blurred on the surface. However, to achieve sharp images with high signal to noise ratio (SNR) the heat flow needs to be controlled in a certain way. That can be done with an amplitude, phase and offset controlled excitation of the surface. This method is based on transferring the temperature contrast measured by the IR camera to an IR projector. Surface areas with a higher temperature are now illuminated with a lower intensity. In addition, the measured phase shift between excitation and detection is compensated for by a time-adjusted excitation. This process takes place iteratively for about 2-10 iterations, whereby the temperature contrast on the component disappears more and more after each iteration, but now reappears more and more clearly in the illumination image of the beamer with a very improved spatial resolution, as the lateral heat flows have been physically eliminated. That means, that the measurement data is now inside the excitation and not as usual in the IR camera. The vanishing lateral gradients convert the problem into a 1D problem, which can be adequately solved by the LT approach. The proposed compensation method can bypass the blind frequency of LT as well and make the inspection largely independent of the excitation frequency. Furthermore, the edge sharpness and separability of features are significantly improved, ultimately improving the feature-detection efficiency. Results have shown, that a SNR increase by a factor of 5 is possible regarding standard LT.

### 2. Fundamentals of 1D-Thermography

Temperature differences are the cause of heat conduction processes in components. If there is a temperature gradient  $\nabla T$ , heat flows from warmer points to colder points according to Fourier's law  $\vec{q} = -\lambda \nabla T$ .

The thermal conductivity  $\lambda$  indicates the relationship between the temperature gradient  $\nabla T$  and the heat flux density  $\vec{q}$  generated by it. The thermal conductivity can be direction-dependent as a second-stage tensor, as is the case with anisotropic composite materials such as carbon fiber reinforced plastics (CFRP), for example. According to [1], the thermal conductivity of a unidirectional CFRP laminate with a fiber content of 25 % by volume was measured to be approximately 13 times greater in the fiber direction than transverse to the fiber direction. For the following investigation, however, the thermal conductivity is assumed to be constant and independent of direction.

For the 1D case (rod or approximately a homogeneous large plate without defects), analytical equations can be used to describe the propagation of thermal waves in solids. Under these assumptions, [2-4] were able to show how layer thicknesses or material inhomogeneities affect the amplitude and phase position of a lock-in thermography measurement. The mathematical description of photothermal effects goes back to the fundamental work of Mandelis [5, 6] and Almond and Patel [7]. Based on this, today's lock-in thermography was developed. Optical lock-in thermography [8, 9] is a test method in active thermography in which a (harmonically) modulated heat source is used to increase the surface temperature of a component. As a response signal, a lock-in evaluation is carried out for each pixel of the thermographic camera - nowadays usually by means of a pixel-by-pixel Fourier transformation. This behaves like a narrowband bandpass filter that only considers signals of the frequency of the (harmonic) excitation. The lock-in evaluation provides two essential pieces of information: phase and amplitude. The phase image shows the delay between the excitation and measurement



signal, while the amplitude image describes the pixel-by-pixel temperature oscillation of the thermal wave in the measurement signal.

In addition to lock-in thermography, there are a large number of measurement and evaluation algorithms for active thermography. These include thermal wave imaging [10], thermal wave imaging radar [11, 12], excitation using Barker Codes [13, 14], using Golay Pairs [15] and 3D tomography of deep-seated defects [16, 17]. All the methods mentioned, including the optical lock-in thermography described above, are based on the pixel-by-pixel evaluation of the measured thermal wave and do not take the lateral heat flow into account in the evaluation. Inhomogeneities are inevitably blurred. The deeper a defect lies, the more blurred it is displayed. The virtual wave concept (VWC), for example, attempts to take this into account. The VWC represents the link between the point heat source in diffusion-free space and the diffused reality. The algorithms applicable to acoustic waves can be applied to the virtual waves determined, thus achieving three-dimensional reconstructions [18]. In the meantime, the one-sided applicability of the method has also been demonstrated [19]. The loss of deformation caused by the reflection arrangement must be compensated for by additional estimates of the boundary conditions for the mathematically complex regularization process. The solution of the poorly posed inverse problem in the virtual wave concept is a mathematically demanding problem, which up to now could only be solved for simple geometries with well-defined boundary conditions.

### 3. Structured Lighting

Structured lighting is another way of taking lateral heat flow into account. The first ideas for spatially structured illumination and interference of thermal waves were implemented as early as 1983. A laser beam was split into two coherent laser beams and the interference of the laser beams in a component was used to obtain depth information of a defect in metallic structures [20]. In [21], the asymmetric heating of the component surface at a moving laser spot was analyzed. Defects and cracks close to the surface could thus be detected with high spatial resolution.

In [22, 23], an LCD presentation projector was used as an optical heat source to implement pixel-by-pixel structured heating for active thermography. Due to the low proportion of thermal radiation, the test surface could only be heated by a few milli-kelvin. In an iterative process, the pixel-by-pixel adjusted phase difference, amplitude difference and mean temperature deviation were compensated for a lock-in measurement in order to obtain a homogeneous measurement result with regard to the pronounced phase and amplitude at a defined excitation frequency of the lock-in measurement. Despite promising results, the phase diverged after a few iterations. It was assumed that this was due to the low excitation power.

In [24, 25], a digital micromirror device (DMD) chip was combined with a near-infrared laser to achieve a structured light source of higher power (20 W input power, 4.4 W optical output power). In the center line of two parallel lines of the same frequency that are 180° out of phase in time, the alternating thermal field was completely canceled out by destructive interference. By observing the center line, disturbances of a homogeneous material (including hidden vertical cracks) could be impressively detected. In [26], a DMD chip and a 30 W near-infrared laser were used to visualize vertical defects by means of targeted structured excitation. The simultaneous projection of two thermal patterns with different modulation frequencies (lock-in excitation at 2 Hz and 2.2 Hz) could be spectrally filtered from the thermogram.

The idea of the compensation method presented here extends the investigations of Holtmann [23] with the focus on a real application for optical lock-in thermography using a heat source of sufficient power.

### 4. Fundamentals of the compensation method

Lateral heat flows inevitably occur after a local temperature change. The local temperature change can be caused, for example, by inhomogeneous heating or inhomogeneous heat conduction defects. The optically excited lock-in thermography measures the local phase shift and the local amplitude of a measuring point in relation to the excitation signal. The measurement signal changes at inhomogeneities, with the local amplitude increasing above inhomogeneities of lower heat capacity (e.g. an air pocket). No trivial statement can be made about the behavior of the phase shift. It behaves differently depending on the defect geometry, heat transfer coefficient, depth position and test frequency and can also vary within a constant depth position. The phase position is strongly influenced by the lateral heat flow. The aim of the compensation method is to specifically reduce the lateral heat flow in the test specimen by adjusting the local excitation. The (local) sinusoidal excitation  $I(x,y,t)$ , equation (1), is divided into three interdependent excitation and measurement parameters for this purpose.

$$I(x, y, t) = \frac{I_{max}}{2} * Off(x, y) + \frac{I_{max}}{2} * Amp(x, y) * \sin(\omega t + \frac{2\pi}{360} Phi(x, y)) \quad (1)$$

$I_{max}$  describes the maximum excitation intensity of the illumination source/test situation,  $Phi(x,y)$  describes the local phase shift of the excitation (An) and measurement signal (Erg),  $Amp(x,y)$  describes the local amplitude of the excitation and measurement signal and  $Off(x,y)$  describes the local uniform heating component of the excitation or the local mean temperature increase in the test specimen due to the excitation.

In the compensation method, the lateral heat flow in the test specimen after excitation is to be minimized by a targeted local adjustment of the three parameters. To achieve this, the influences of the inhomogeneity of the test specimen

are to be projected onto the virtual plane of the excitation. The targeted local adaptation of the excitation parameters then contains the desired defect information for a homogeneous response signal ( $Phi_{Erg}$ ,  $Amp_{Erg}$  and  $Off_{Erg}$ ). It should be noted that perfect compensation on non-homogeneous structures is only possible with the trivial solution  $Amp_{An} = Off_{An} = 0$ . In the non-homogeneous case, a local temperature gradient inevitably occurs due to inhomogeneous excitation, which in turn induces a lateral heat flow.

In an iterative process, this local temperature gradient is to be reduced within the compensation method by adjusting the local excitation parameters  $Phi_{An}$ ,  $Amp_{An}$ ,  $Off_{An}$ . Since lateral heat flows are inevitably induced by inhomogeneous excitation, the local temperature gradients occurring over time are not minimized, but the measurement parameters  $Phi_{Erg}$ ,  $Amp_{Erg}$  and  $Off_{Erg}$  are homogenized. The more homogeneous these three measurement parameters of the lock-in measurement are, the lower the local temperature gradients averaged over the measurement periods and thus also the lateral heat flows. The proportion of uniform heating caused by  $Off_{An}$  is compensated for linearly. The resulting temperature field  $T(x,y,t)$  on the surface of the test specimen is evaluated using a discrete Fourier transformation. The local measurement parameters  $Phi_{Erg}$  and  $Amp_{Erg}$  are formed from this.  $Off_{Erg}$  is determined from the time average of the last linearly compensated measurement period.

## 5. Procedure of the compensation method

For the first iteration of the compensation method, a classic optical lock-in thermography test is performed.  $Phi_{An}$  is assumed to be 0,  $Amp_{An}$  and  $Off_{An}$  are selected to an amount suitable for the test situation. This should be sufficiently large to achieve a thermal contrast around the component (cf. perfect compensation with  $Amp_{An} = Off_{An} = 0$ ) and not too large so that the component heats up too much and the convective and radiation-related part of the heat transfer is reduced. As a result of the lock-in thermography test, the values  $Phi_{Erg}$ ,  $Amp_{Erg}$  and  $Off_{Erg}$  are now obtained for iteration 0. The local excitation parameters for the subsequent iteration are determined based on the results. The excitation phase  $Phi_{An, i+1}$  is trivially corrected. The respective difference between the previous excitation and the previous result is taken into account for the subsequent iteration. For the amplitude and offset, the subsequent excitation amplitude and excitation offset are reduced by the factor by which the local amplitude/offset is greater than the smallest amplitude/offset in the result. This process causes the amplitude and offset to decrease with each successive iteration. The limit value of the optimization loop thus converges to the trivial solution  $Amp_{An, \infty} = Off_{An, \infty} = 0$ .  $Phi_{An, \infty}$  is undetermined.  $Phi_{An, i+1}$  and  $Amp_{An, i+1}$  are thus iterated as described by Holtmann in [23] and are given in equations (2) and (3). A different iteration is used for the excitation offset  $Off_{An, i+1}$ . Since the offset must always be greater than the amplitude, the local excitation offset is formed as the maximum value of the determined excitation offset and the excitation amplitude, see equations (4) and (5). Due to this description, no convergence problems occurred in the investigations.

$$Phi_{An, i+1} = Phi_{An, i} - Phi_{Erg, i} \quad (2)$$

$$Amp_{An, i+1} = Amp_{An, i} * \frac{\min(Amp_{Erg, i})}{Amp_{Erg, i}} \quad (3)$$

$$Off_{An, i+1} = Off_{An, i} * \frac{\min(Off_{Erg, i})}{Off_{Erg, i}} \quad (4)$$

$$Off_{An, i+1} = \max(Amp_{An, i+1}, Off_{An, i+1}) \quad (5)$$

## 6. Implementation of the compensation method

The compensation method is implemented using the finite element software COMSOL Multiphysics, COMSOL AB, Stockholm, Sweden. For this purpose, a test specimen of the size 150 mm x 100 mm x 6 mm, a density of 1620 kg/m<sup>3</sup>, a constant heat capacity of 892 J/(kg K) and a thermal conductivity of 0.6 W/(m K) is created and provided with different internal geometries. Depth information of the inner geometries is shown in Fig. 1. Grooves 12 mm long and 2 mm wide with a spacing of 6 mm are made in the test specimen (Fig. 1 above). The residual wall thickness of the grooves from top to bottom is 1 mm, 2 mm and 3 mm. Flat-bottom holes with a diameter of 1 mm to 5 mm were drilled symmetrically in between. The letters I, K and T with residual wall thicknesses of 0.5 mm, 1.5 mm and 2.5 mm were inserted into the test specimen in Fig. 1 below. The bars of the letters have a width of 10 mm.

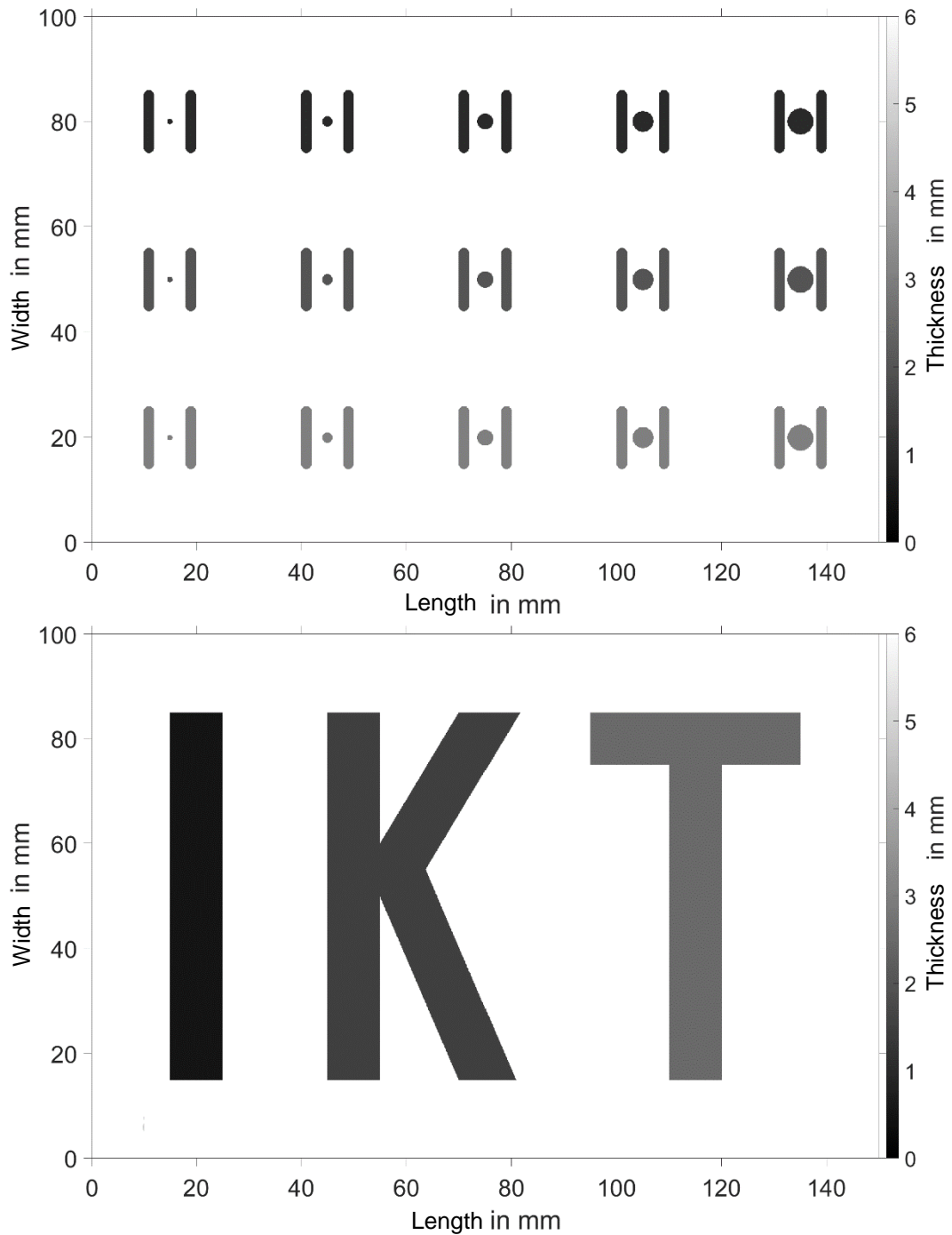


Figure 1: Illustration of the internal geometries, top: Groove geometry with intermediate flat bottom holes and residual wall thicknesses of 1 mm, 2 mm and 3 mm, bottom: IKT lettering with residual wall thicknesses of 0.5 mm, 1.5 mm and 2.5 mm

The heating takes place over the entire surface of the homogeneous test specimen and is excited according to equation (1) with a locally variable sinusoidal heat source. The maximum intensity  $I_0$  of the illumination source is defined as  $800 \text{ W/m}^2$ . In relation to the component surface, this corresponds to a maximum power of 12 W. The inclusions and the rear wall are regarded as thermal insulators and the lateral surfaces are described as symmetrical edge conditions. A convective heat flow of  $5 \text{ W/(m}^2 \text{ K)}$  is assumed on the top of the test specimen. The mesh is formed with a free tetrahedral mesh of size 1 mm (mesh refinement on thin structures up to 0.33 mm) and square seridipity elements. The simulation is performed at an excitation frequency of 0.01 Hz and a relative accuracy of  $10^{-8}$  for two periods. 20 time steps are exported per period.

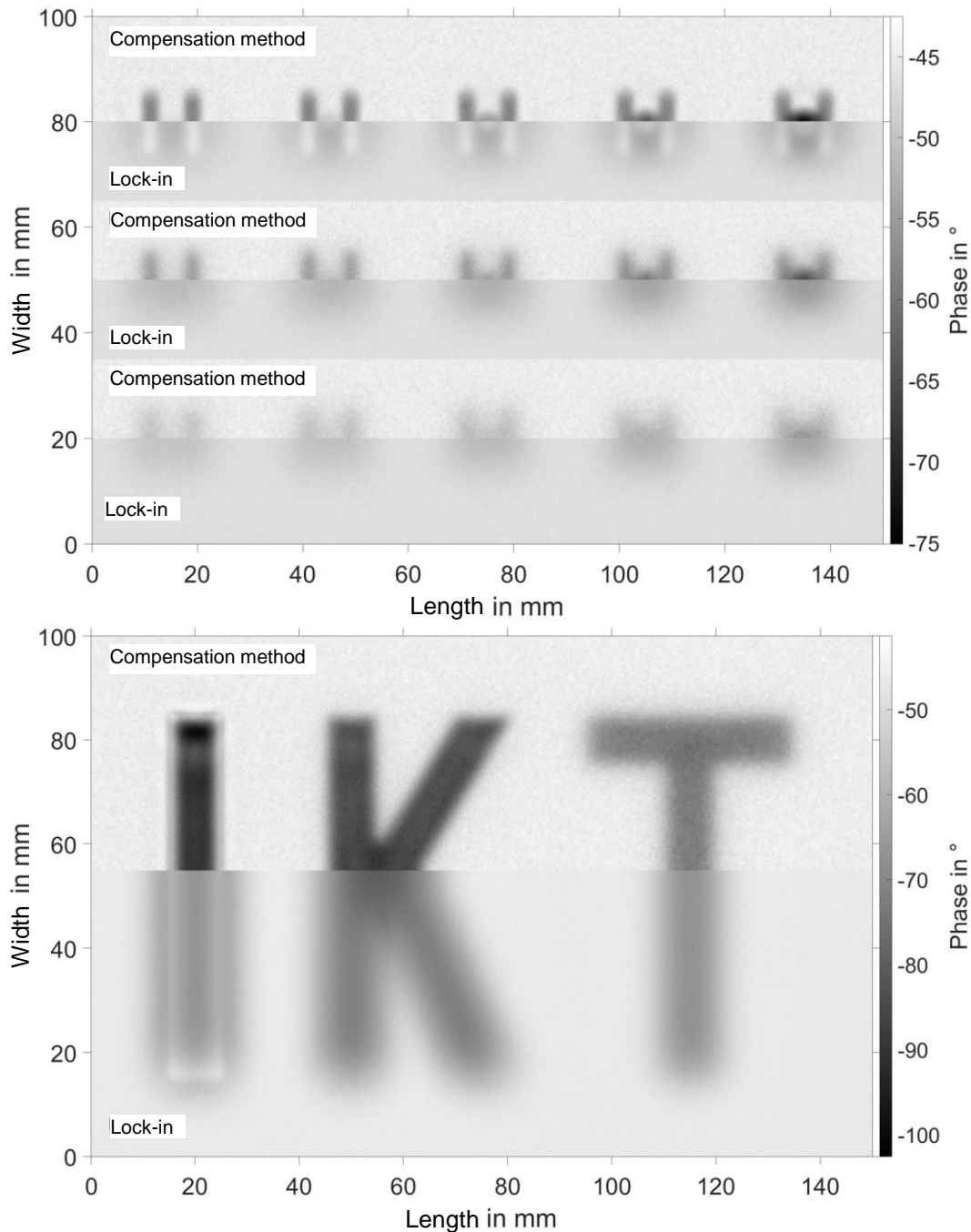


Figure 2: Results of lock-in thermography and the compensation method (10th iteration) for the geometries shown in Fig. 1. Top: Groove geometry with flat bottom holes, bottom: IKT lettering

The evaluation described above is carried out exclusively on the second period. The resulting temperature field is superimposed with a uniformly distributed 20 mK<sub>PP</sub> temperature noise before evaluation. For the present case, the compensation method is carried out in ten iterations and the results of the first iteration (classic lock-in thermography) are compared with the excitation of the tenth iteration (result of the compensation method). This is shown for the two geometries in Fig. 2. The measurement result was divided into areas for lock-in thermography and areas for the compensation method. These are marked in the figure. As can be clearly seen, the image sharpness increases with the compensation method. Defects are more clearly separated from each other and different depth structures (IKT lettering, different phase values) can also be separated in a more targeted manner.

To investigate the separability of closely spaced defects, two squares with an edge length of 2 mm were examined at a depth of 1 mm at different positioning distances from each other using the compensation method. The distances between the two squares were increased in 0.1 mm steps from 0 mm (rectangle of length 4 mm × 2 mm) up to a distance of 4 mm, Fig. 3, right. In the following, the phase curves at the recorded intersection line through the two squares are

viewed over the distance, see Fig. 3, left. Fig. 4 clearly shows that the compensation method can separate closely spaced defects very well. A reduced phase value between the two squares is detected in the compensation method from an edge distance of just 0.4 mm.

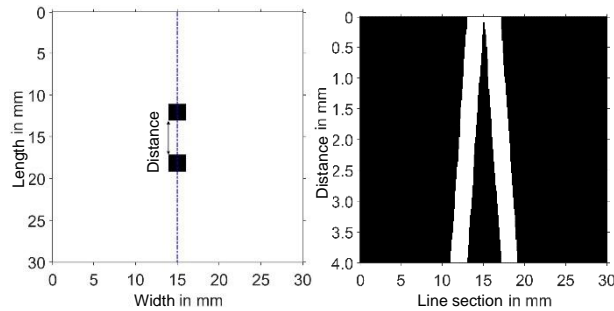


Figure 3: Geometries of the distance analysis, left: Geometry of the squares at 4 mm distance, right: line intersections through symmetry plane at different distances

With classic lock-in thermography, however, the phase reduction only occurs from an edge distance of 1.9 mm. Another side effect is that the useful signals at the defect (square in Fig. 4 or depth structure in Fig. 2) form a higher contrast to the noise signal. A disadvantage is that the compensation method introduces increased noise into homogeneous areas.

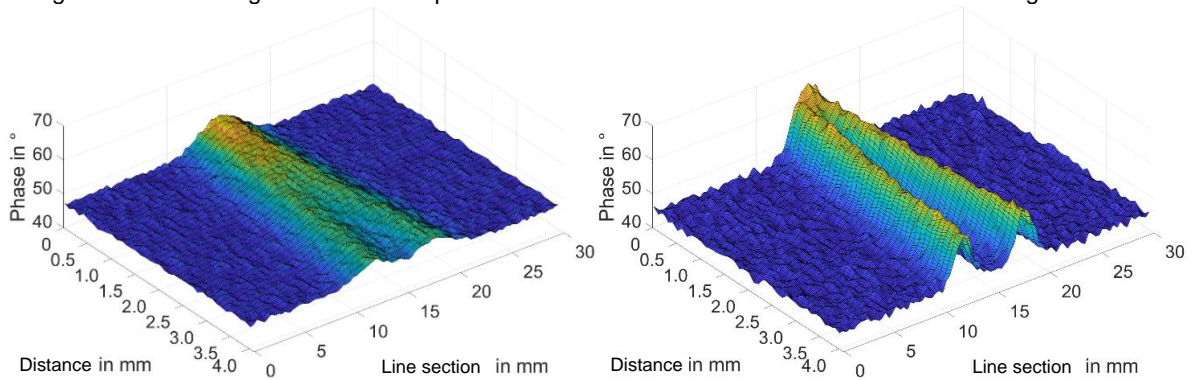


Figure 4: Line section of the phase values with different edge distances of the squares. Left: Lock-in thermography, right: compensation method

## 7. Conclusion and outlook

The compensation method presented reliably reduces the lateral heat flows of a lock-in thermography measurement and transfers them to the excitation source. Defect geometries appear sharper in the new response signal (the phase excitation of the illumination source) and can be separated more precisely from closely adjacent defects. At a depth of 1 mm, the compensation method was able to reduce the distance between two squares (edge length 2 mm) from 1.9 mm (classic lens thermography) to 0.4 mm. Thanks to the optimized iteration equations, the compensation method could be carried out without convergence problems or other limitations. The reason for the increased noise on homogeneous structures is suspected in the simulation, but is to be confirmed by validation measurements. As part of the research project, it is planned to replicate the excitation source in the future and to validate the promising simulation results by means of experiments.

## 8. Acknowledgments

The results presented here were produced within the framework of the research project 470535306 funded by the German Research Foundation (DFG).

## REFERENCES

- [1] INCROPERA, F.P., D.P. DEWITT, T.L. BERGMAN UND A.S. LAVINE. Fundamentals of heat and mass transfer. 2007. ISBN 9780471457282.
- [2] KARPEN, W. Berührungslose und zerstörungs-freie Prüfung von Kunststofflackierungen mit thermischen Wellen. Dissertation. Stuttgart, 1993.
- [3] SPIEßBERGER, C. Merkmalsanalyse mit thermischen Wellen in der zerstörungsfreien Werkstoff- und Bauteilprüfung. Dissertation, 2012. Doi:10.18419/opus-1992
- [4] BENNETT, C.A. UND R.R. PATTY. Thermal wave interferometry: a potential application of the photoacoustic effect. In: Applied optics, 1982, 21(1), 49–54. Doi:10.1364/AO.21.000049
- [5] MANDELIS, A. Photoacoustic and thermal wave phenomena in semiconductors. New York: North-Holland, 1987. ISBN 0444012265.
- [6] MANDELIS, A. Diffusion-Wave Fields. Mathematical Methods and Green Functions. New York, NY: Springer New York, 2001. ISBN 9781475735482.
- [7] ALMOND, D. UND P. PATEL. Photothermal science and techniques. London: Chapman & Hall, 1996. Physics and its applications. 10. ISBN 0412578808.
- [8] BREITENSTEIN, O., W. WARTA UND M.C. SCHUBERT. Lock-In Thermography. Basics and Use for Evaluating Electronic Devices and Materials. 3rd ed. Cham: Springer, 2019. Springer Series in Advanced Microelectronics Ser. v. 10. ISBN 978-3-319-99825-1.
- [9] WU, D. Lock-in-Thermographie für die zerstörungsfreie Werkstoffprüfung und Werkstoffcharakterisierung. Dissertation. Stuttgart, 1996.
- [10] MULAVEESALA, R. UND S. TULI. Theory of frequency modulated thermal wave imaging for nondestructive subsurface defect detection. In: Applied Physics Letters, 2006, 89(19), 191913. Doi:10.1063/1.2382738
- [11] TABATABAEI, N. UND A. MANDELIS. Thermal-wave radar: a novel subsurface imaging modality with extended depth-resolution dynamic range. In: The Review of scientific instruments, 2009, 80(3), 34902. Doi:10.1063/1.3095560
- [12] TABATABAEI, N. UND A. MANDELIS. Thermal-wave radar. In: Journal of Physics: Conference Series, 2010, 214, 12088. Doi:10.1088/1742-6596/214/1/012088
- [13] GHALI, V.S., S.S.B. PANDA UND R. MULAVEESA-LA. Barker coded thermal wave imaging for defect detection in carbon fibre-reinforced plastics. In: Insight - Non-Destructive Testing and Condition Monitoring, 2011, 53(11), 621–624. Doi:10.1784/insi.2011.53.11.621
- [14] SHI, Q., J. LIU, W. LIU, F. WANG UND Y. WANG. Barker-coded modulation laser thermography for CFRP laminates delamination detection. In: Infrared Physics & Technology, 2019, 98, 55–61. Doi:10.1016/j.infrared.2019.02.007
- [15] ARORA, V. UND R. MULAVEESALA. Application of golay complementary coded excitation schemes for non-destructive testing of sandwich structures. In: Optics and Lasers in Engineering, 2017, 93, 36–39. Doi:10.1016/j.optlaseng.2017.01.009
- [16] KAIPILAVIL, S. UND A. MANDELIS. Truncated-correlation photothermal coherence tomography for deep subsurface analysis. In: Nature Photonics, 2014, 8(8), 635–642. Doi:10.1038/nphoton.2014.111
- [17] TAVAKOLIAN, P., K. SIVAGURUNATHAN UND A. MANDELIS. Enhanced truncated-correlation photothermal coherence tomography with application to deep subsurface defect imaging and 3-dimensional reconstructions. In: Journal of Applied Physics, 2017, 122(2), 23103. Doi:10.1063/1.4992807
- [18] BURGHOLZER, P., M. THOR, J. GRUBER UND G. MAYR. Three-dimensional thermographic imaging using a virtual wave concept. In: Journal of Applied Physics, 2017, 121(10), 105102. Doi:10.1063/1.4978010
- [19] THUMMERER, G., G. MAYR, P.D. HIRSCH, M. ZIEGLER UND P. BURGHOLZER. Photothermal image reconstruction in opaque media with virtual wave backpropagation. In: NDT & E International, 2020, 112, 102239. Doi:10.1016/j.ndteint.2020.102239
- [20] BUSSE, G. UND K.F. RENK. Stereoscopic depth analysis by thermal wave transmission for non-destructive evaluation. In: Applied Physics Letters, 1983, Doi:10.1063/1.93942
- [21] SCHLICHTING, J., C. MAIERHOFER UND M. KREUTZBRUCK. Crack sizing by laser excited thermography. In: NDT&E International, 2012, 133–140. Doi:10.1016/j.ndteint.2011.09.014
- [22] HOLTSMANN, N., K. ARTZT, A. GLEITER, H.P. STRUNK UND G. BUSSE. Iterative improvement of Lock-in-thermography results by temporal and spatial adaptation of optical excitation. In: Quantitative InfraRed Thermography Journal, 2012, 9(2), 167–176. Doi:10.1080/17686733.2012.741919
- [23] HOLTSMANN, N. Auswertung und Anregung eindimensionalen Wärmeflusses in der zerstörungsfreien Bauteilprüfung mittels optisch angeregter Lock-in-Thermografie. Dissertation. München: Dr. Hut, 2015. Luftfahrt. ISBN 978-3-8439-2222-7.
- [24] THIEL, E. Thermische Wellenformung für interferenzbasierte thermografische Defektdetektion. Dissertation: Universität Stuttgart, 2020.
- [25] THIEL, E., M. KREUTZBRUCK UND M. ZIEGLER. Spatial and temporal control of thermal waves by using DMDs for interference based crack detection. In: M.R. DOUGLASS, P.S. KING und B.L. LEE, Hg. Emerging Digital Micromirror Device Based Systems and Applications VIII: SPIE, 2016, 97610N, doi:10.1117/12.2210918.

- [26] PRIBE, J.D., S.C. THANDU, Z. YIN UND E.C. KIN-ZEL. Toward DMD illuminated spatial-temporal modulated thermography. In: J.N. ZALAMEDA und P. BISON, Hg. Thermosense: Thermal Infra-red Applications XXXVIII: SPIE, 2016, 98610, DOI:10.1117/12.2223859.